Hybrid Beamforming in Uplink Massive MIMO Systems in the Presence of Blockers

Xinlin Zhang*, Mikael Coldrey*†, Thomas Eriksson*, and Mats Viberg*
* Department of Signals and Systems, Chalmers University of Technology, Gothenburg, Sweden
† Ericsson Research, Ericsson AB, Gothenburg, Sweden
E-mail: xinlin@chalmers.se, mikael.coldrey@ericsson.com, {thomase, mats.viberg}@chalmers.se

***Abstract*—Hybrid beamforming (HBF) is a potential solution to reduce the baseband hardware cost in massive multiple-input multiple-output (MIMO) systems that has drawn considerable attention recently. In this paper, we consider the uplink of a multiuser massive MIMO system in the presence of blockers. Such blockers, which arise from, for example, users served by other non-cooperative base stations (BSs), can limit the system performance if not handled properly. We propose a HBF scheme that can remove the impact of blockers, while preserving signals from intended users. Specifically, in our two-step receive beamforming scheme, the analog beamformer (ABF) is designed based on channel covariance matrices to minimize the powers of blockers, while the digital beamformer (DBF) deals with inter-user interference. We propose an iterative algorithm that efficiently gives a good sub-optimal solution to the NP-hard problem in the ABF design. Moreover, we consider a more complete BS architecture by incorporating automatic gain control (AGC) and analog-to-digital converter (ADC). As we show in the simulations, for a system with full-precision ADCs, our scheme approaches the sum rate of an ideal fully-digital system. Interestingly, for a system with low-resolution ADCs, our HBF scheme can even outperform a fully-digital system.**

I. Introduction

Massive multiple-input multiple-output (MIMO) system is envisioned as a key enabler to meet the exponentially growing data demand in future wireless communication networks. It has been shown that, by deploying $M \gg 1$ antennas at the base stations (BSs), massive MIMO can offer huge improvement in spectral efficiency with simple linear processing schemes, such as matched-filtering (MF) and zero-forcing (ZF) [1]. Nevertheless, the cost of building such a system is still prohibitive if each of the M antennas is connected to an individual digital chain. Recently, a hybrid BS architecture has been proposed to reduce the cost by adopting a two-stage beamforming scheme [2], [3]. Specifically, such a hybrid architecture splits the beamforming into analog and digital domains, where the analog beamforming is realized by a power-efficient and cost-effective phase-shifter network, which reduces the required number of digital chains from M to N ($N \leq M$). In principle, introducing the additional analog beamforming (ABF) and limiting the number of digital chains may degrade the system performance. However, due to the limited local scattering nature of MIMO channels, the number of active channel eigenmodes may be much less than M [4], [5]. Thus, if the ABF is properly designed, the performance degradation may be negligible [6].

There are a few existing works on hybrid beamforming (HBF), which cover both mmWave and low-frequency channels [2], [3], [6]–[10]. The pioneering work [2] provides a low-complexity hybrid precoding design algorithm, by exploiting the sparse nature of mmWave channels. Then, [3] extends the work in [2] to the case when only partial channel state information (CSI) is available. A novel bi-convex approximation approach is proposed in [6] in order to design the HBF, such that the minimum achievable rates of users can be maximized. In [8], the authors propose a simple MF-like HBF scheme for low-frequency channels under the assumption of perfect CSI. Channel estimation with hybrid BS architectures have been addressed in [8], [9]. Recently, low-resolution analog-to-digital converters (ADCs) have also been brought into the framework of HBF [10], where a comprehensive study on the trade-off between energy efficiency and spectral efficiency is presented.

In this paper, we study the receive HBF design in the uplink of a single-cell multiuser massive MIMO system. In contrast to prior works, we consider a practical scenario with blockers presenting in the system. These blockers can be caused by unscheduled users, intentional jammers, etc.; and they can cause a substantial interference.[1] Engineers believe that a robust system should be able to handle blockers that are up to 60 dB stronger than the signal of interest (SOI). Besides blockers, we also consider a more complete system architecture by incorporating two essential components: automatic gain control (AGC) and ADC. AGC rescales the received signal such that it fits the dynamic range of the ADC, while the ADC quantizes the continuous signals into discrete values. In such a system, blockers may severely distort the SOI, hence we aim to remove as much as possible the blockers in the analog domain. Specifically, formulate the ABF design as a max signal-to-noise-plus-interference ratio (SINR) problem, subject to the constant modulus constraint that arises from the nature of fixed-gain phase shifters used by the ABF. Based on the work of unimodular programming (UQP) [11], we propose a two-step iterative algorithm that can efficiently provide a good sub-optimal solution to this optimization problem, which

[1] One simple example would be the following: two closely spaced users operating at the same time/frequency are served by two non-cooperative BSs, while user-1 is served by BS-1 and user-2 is served by BS-2. If user-1 is close to BS-1, but user-2 is on the cell edge of BS-2, then, with uplink power control, the transmit power of user-2 will be much larger than user-1, such that the signal of MS-1 can be blocked at BS-1.

is in general NP-hard. Our simulation results show that, for systems with full-precision ADCs, our scheme approaches the sum rate achieved by ideal and fully digital systems, with only marginal degradation. For systems with low resolution ADCs, our HBF scheme can even outperform fully digital systems. This counter-intuitive result is mainly due to the impact of blockers and the joint effects of AGC and ADC, which will be discussed in more detail in the paper.

Notation: Upper and lower case boldface letters denote matrices and vectors, respectively. The $n \times n$ identity matrix is represented by $\mathbf{I}_n$. The superscripts $(\cdot)^H$ and $(\cdot)^{-1}$ stand for Hermitian transposition and matrix inverse, respectively. The symbol $\mathcal{CN}(\mathbf{m}, \mathbf{\Sigma})$ denotes a multi-variate circularly-symmetric complex Gaussian (CSCG) distribution with mean $\mathbf{m}$ and covariance $\mathbf{\Sigma}$. For any matrix $\mathbf{H} \in \mathbb{C}^{m\times n}$, $\mathbf{h}_i$ is the i-th column of $\mathbf{H}$. The element-wise exponentiation of matrix $\mathbf{A}$ is denoted by $e^{\mathbf{A}}$, and $\arg(\mathbf{A})$ returns the element-wise phases of matrix $\mathbf{A}$.

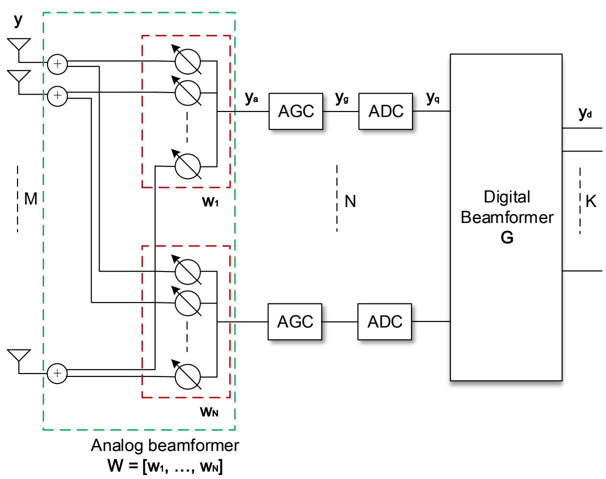

Fig. 1. Hybrid BS architecture.

II. System and Signal Models

We consider the uplink of a single-cell multiuser massive MIMO system, where the BS is equipped with M antennas and simultaneously serves K single-antenna users. The received signal $\mathbf{y} \in \mathbb{C}^{M\times 1}$ at the BS can then be expressed as

$$\mathbf{y} = \mathbf{H}\mathbf{x} + \mathbf{H}_b\mathbf{x}_b + \mathbf{n}, \tag{1}$$

where $\mathbf{x} \in \mathbb{C}^{K\times 1}$ and $\mathbf{x_b} \in \mathbb{C}^{K_b\times 1}$ concatenate the signals transmitted by all K users and all K_b blockers, respectively, where K_b is unknown. The additive white Gaussian noise (AWGN) is represented by $\mathbf{n} \in \mathbb{C}^{M\times 1} \sim \mathcal{CN}(0, \mathbf{I}_M)$. We denote $\mathbf{H} = [\mathbf{h}_1\ \mathbf{h}_2\ \ldots\ \mathbf{h}_K] \in \mathbb{C}^{M\times K}$ as the channel between the K users and the BS, while we use $\mathbf{H}_b$ as the channel of blockers.

The channel of user k, denoted by $\mathbf{h}_k$, is modeled as $\mathbf{h}_k = \mathbf{R}_k^{\frac{1}{2}}\boldsymbol{\alpha}_k$, $\forall k = 1, \ldots, K$, where $\boldsymbol{\alpha}_k \in \mathbb{C}^M$ has i.i.d. CSCG entries with zero mean and unit variance; and $\mathbf{R}_k \in \mathbb{C}^{M\times M}$ is the corresponding spatial correlation matrix. For massive MIMO systems, the rank of $\mathbf{R}_k$, denoted by r_k, may be much smaller than M [5], [6], therefore we can alternatively represent $\mathbf{h}_k$ as

$$\mathbf{h}_k = \mathbf{U}_k\mathbf{\Lambda}_k^{\frac{1}{2}}\mathbf{a}_k, \tag{2}$$

where $\mathbf{\Lambda}_k$ is an $r_k \times r_k$ diagonal matrix whose diagonal elements are the nonzero eigenvalues of $\mathbf{R}_k$, while $\mathbf{U}_k \in \mathbb{C}^{M\times r_k}$ contains the corresponding eigenvectors; $\mathbf{a}_k \in \mathbb{C}^{r_k}$ is truncated from $\boldsymbol{\alpha}_k$, thus each of its elements also follows $\mathcal{CN}(0,1)$.

As shown in Fig.1, the received signal $\mathbf{y}$ is firstly weighted by the ABF matrix $\mathbf{W} \in \mathbb{C}^{M\times N}$, and each of the N outputs is fed into AGC and then ADC. Finally, the quantized signals are processed by DBF at the baseband. Specifically, the signal after each processing step can be expressed as shown below.
After ABF:

$$\mathbf{y}_{\mathrm{a}} = \mathbf{W}^H\mathbf{y}. \tag{3}$$

After AGC:

$$\mathbf{y}_g = \mathrm{diag}(\mathbf{c})\mathbf{y}_{\mathrm{a}}, \tag{4}$$

where $\mathbf{c}_i = \sqrt{\frac{c}{P_{\mathbf{y}_{a\,i}}}}, \forall i = 1, \ldots, N$, rescales the power of the ith element of $\mathbf{y}_a$ such that the output power satisfies the dynamic range of the corresponding ADC.
After ADC:

$$\mathbf{y}_q = Q(\mathbf{y}_q) = \kappa\mathbf{y}_g + \mathbf{n}_q, \tag{5}$$

where $Q(\cdot)$ is the quantization operation performed by the ADCs, and $\mathbf{n}_q$ models the additive quantization noise. A uniform linear quantizer will be assumed, such that $\mathbf{y}_g$ and $\mathbf{n}_q$ are (approximately) uncorrelated [12], and that $\mathbf{n}_q$ has mean $\mathbf{0}$, and variance $\kappa(1-\kappa)\sigma^2_{\mathbf{y}_g}$, where κ is a real scalar that depends on the type of ADC, and $\sigma^2_{\mathbf{y}_g}$ is the variance of the corresponding input to the ADCs. This is in accordance with the additive quantization noise model (AQNM) in [12].
Finally, after DBF, the signal is recovered as

$$\begin{aligned}\mathbf{y}_d &= \mathbf{G}^H\mathbf{y}_q, &(6)\\ &= \mathbf{G}^H(\kappa\mathbf{y}_g + \mathbf{n}_q), &(7)\\ &= \mathbf{G}^H(\kappa\mathrm{diag}(\mathbf{c})\mathbf{y}_a + \mathbf{n}_q), &(8)\\ &= \mathbf{G}^H(\kappa\mathrm{diag}(\mathbf{c})\mathbf{W}^H\mathbf{y} + \mathbf{n}_q), &(9)\\ &= \mathbf{G}^H(\mathbf{H}_{\mathrm{eq}}\mathbf{x} + \mathbf{n}_{\mathrm{eq}}), &(10)\end{aligned}$$

where $\mathbf{n}_{\mathrm{eq}} \triangleq \kappa\mathrm{diag}(\mathbf{c})\mathbf{W}^H(\mathbf{H}_b\mathbf{x}_b + \mathbf{n}) + \mathbf{n}_q$ is the total effective noise, and $\mathbf{H}_{\mathrm{eq}} = \kappa\mathrm{diag}(\mathbf{c})\mathbf{W}^H\mathbf{H}$ is the effective channel seen at the baseband. The DBF $\mathbf{G}$ is then designed based on $\mathbf{H}_{\mathrm{eq}}$. Thanks to the reduced dimension, $\mathbf{H}_{\mathrm{eq}}$ can be estimated using conventional techniques, such as least-square (LS) estimation or minimum mean-square error (MMSE) estimation. For brevity, we assume that $\mathbf{H}_{\mathrm{eq}}$ is known at the baseband.

III. Problem Formulation

In this paper, we consider the special case $N = K$, i.e., we use the minimum number of digital chains required in the BS. Extension to the general case $N > K$ will be studied in future work. As explained in Section II, we consider blockers' presence in the system, and both AGC and ADC are incorporated in the BS architecture. The joint effect of AGC and ADC is illustrated in Fig.2, where the areas of green and red blocks denote the powers of SOI and blockers plus AWGN, respectively. AGC rescales the input signal power to fit the dynamic range of the ADC, denoted by the black box, while preserving the ratio between SOI and blockers plus AWGN. Then, this rescaled signal is fed into the ADC, where a scaled version of the input signal is produced with additive quantization noise, as we have explained in Section II. As one can envision, if blockers are not removed properly, the SOI that remains in the end may be overwhelmed by the quantization noise. Therefore, before entering AGC, it is crucial to design an ABF that can remove the impact of blockers as much as possible.

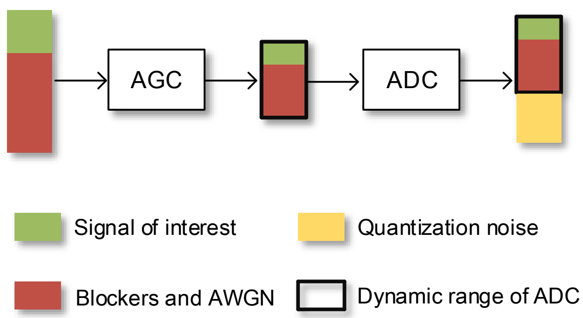

Fig. 2. Illustration of the joint effect of AGC and ADC.

In light of this, we design the ABF $\mathbf{W} \triangleq [\mathbf{w}_1 \ldots \mathbf{w}_K]$ according to the following max-SINR criterion:

$$\begin{aligned}(\mathrm{P1}): \ \max_{\mathbf{w}_k} \ & \frac{\mathbf{w}_k^H \mathbf{R}_k \mathbf{w}_k}{\mathbf{w}_k^H \mathbf{R}_I \mathbf{w}_k} \\ \text{s.t. } & \mathbf{w}_k \in \mathcal{CM},\end{aligned}$$

for $k = 1, \ldots, K$, where $\mathcal{CM}$ denotes the set of vectors/matrices that satisfy the unit constant modulus constraint, i.e., $\mathcal{CM} = \{\mathbf{A} \in \mathbb{C}^{m \times n} \big| |\mathbf{A}_{i,j}| = 1, \forall i = 1, \ldots, m, j = 1, \ldots, n\}$, while $\mathbf{R}_I \triangleq \mathbf{R}_b + \mathbf{I}_M$ is the covariance matrix of blockers plus AWGN. In this paper, we assume that the channel covariance matrices $\mathbf{R}_k$ are known, and that $\mathbf{R}_y$, the covariance matrix of the received signal, can be measured [13]. Thus, we can directly obtain $\mathbf{R}_I$ by subtracting $\sum_{i=1}^{K} \mathbf{R}_i$ from $\mathbf{R}_y$, i.e., $\mathbf{R}_I = \mathbf{R}_y - \sum_{i=1}^{K} \mathbf{R}_i$. It can be observed that our aim is to maximize the proportion of SOI after AGC processing.

Please note that if we discard the constant modulus constraint, the solution to (P1) can be found by solving the generalized eigenvalue problem

$$\mathbf{R}_I \mathbf{w}_k = \lambda \mathbf{R}_k \mathbf{w}_k, \tag{11}$$

and the optimal beamformer $\mathbf{w}_k$ is given by the eigenvector that corresponds to the smallest generalized eigenvalue of the matrix pencil $\{\mathbf{R}_I, \mathbf{R}_k\}$, which is known as the generalized Capon (G-Capon) beamformer [14]. However, it can be proved that the constant modulus constraint imposes NP-hardness to (P1), which makes finding the global optimal solution prohibitive [15]. Hence, in the following, we resort to find good sub-optimal solutions.

IV. Algorithm To Solve (P1)

In this section, we present our iterative algorithm that solves (P1) in two steps.

In the first part, we focus on the problem below:

$$\begin{aligned}(\mathrm{P2}): \ \max_{\mathbf{w}} \ & \mathbf{w}^H \mathbf{R} \mathbf{w} \\ \text{s.t. } & \mathbf{w} \in \mathcal{CM},\end{aligned}$$

where $\mathbf{R}$ is some symmetric positive semidefinite matrix, and $\mathbf{w} \in \mathbb{C}^{M \times 1}$ is the unit modulus vector that maximizes the quadratic form $\mathbf{w}^H \mathbf{R} \mathbf{w}$. Despite its NP-hardness, there exists polynomial time approximations that give good sub-optimal solutions, e.g., Gaussian randomization technique [15]; however, this method is not scalable as M goes large. Recently, a so-called power-iteration method has been applied to tackle this problem, which can effieciently provide a good solution [11]. This algorithm is summarized in the following lemma:

Lemma 1: Let $\mathbf{w}^{(t+1)} = e^{j \cdot \arg\left(\mathbf{R}\mathbf{w}^{(t)}\right)}$, where $t = 0, 1, \ldots$ denotes the index of iteration. Then, given an arbitrary staring point $\mathbf{w}^{(0)}$, $\mathbf{w}^{(t)}$ converges to a local optimum of (P2) as $t \to \infty$.

Proof: A detailed proof can be found in [11]. ∎

Basically, this algorithm ensures that ${\mathbf{w}^{(t+1)}}^H \mathbf{R} \mathbf{w}^{(t)}$ is monotonically increasing in each iteration. Moreover, it is also observed that the quadratic objective function in (P2) is upper bounded by the sum of absolute values of each element in $\mathbf{R}$. Therefore, convergence is always guaranteed.

In the second part of our algorithm, we resort to the Dinkelback's approach [16], and start by defining a new function $f(\mathbf{w})$ as

$$f(\mathbf{w}) \triangleq \frac{a(\mathbf{w})}{b(\mathbf{w})}, \tag{12}$$

where $a(\mathbf{w}) = \mathbf{w}^H \mathbf{R}_\mathrm{I} \mathbf{w}$ and $b(\mathbf{w}) = \mathbf{w}^H \mathbf{R} \mathbf{w}$, the user index k is dropped at this stage for simplicity. It can be seen that the objective function in $(P1)$ is precisely $\frac{1}{f(\mathbf{w})}$, thus, maximizing the SINR is equivalent to minimizing $f(\mathbf{w})$. Next, we define another function

$$g(\mathbf{w}, \mathbf{w}_c) \triangleq a(\mathbf{w}) - f(\mathbf{w}_c) b(\mathbf{w}) = \mathbf{w}^H \left(\mathbf{R}_\mathrm{I} - f(\mathbf{w}_c)\mathbf{R}\right) \mathbf{w}, \tag{13}$$

where $\mathbf{w}_c$ denotes some known value of $\mathbf{w}$. It can be easily verified that $g(\mathbf{w}_c, \mathbf{w}_c) = 0$. Furthermore, let

$$\mathbf{w}^\star = \operatorname*{argmin}_{\mathbf{w} \in \mathcal{CM}} g(\mathbf{w}, \mathbf{w}_c), \tag{14}$$

then, we have

$$g(\mathbf{w}^\star, \mathbf{w}_c) = a(\mathbf{w}^\star) - f(\mathbf{w}_c) b(\mathbf{w}^\star) \leq g(\mathbf{w}_c, \mathbf{w}_c) = 0. \tag{15}$$

Hence, for any $b(\mathbf{w}^\star) \neq 0$, we observe that $f(\mathbf{w}^\star) \leq f(\mathbf{w}_c)$, i.e., we can iteratively replace $\mathbf{w}_c$ with the current optimal value $\mathbf{w}^\star$, until $f(\mathbf{w})$ reaches its minimum.[2] Now, let $\lambda_{\max}$ be the largest eigenvalue of $\mathbf{R}_{\mathrm{I}} - f(\mathbf{w}_c)\mathbf{R}$, and define $\tilde{\mathbf{R}} \triangleq \lambda_{\max}\mathbf{I}_M - (\mathbf{R}_{\mathrm{I}} - f(\mathbf{w}_c)\mathbf{R})$, it follows readily that $\tilde{\mathbf{R}}$ is positive semidefinite. Moreover, it is straightforward to show that $\mathbf{w}^\star$ in (14) is identical to the following

$$\mathbf{w}^\star = \underset{\mathbf{w}\in\mathcal{CM}}{\operatorname{argmax}}\ \tilde{g}(\mathbf{w}, \mathbf{w}_c), \tag{16}$$

where $\tilde{g}(\mathbf{w}) \triangleq \mathbf{w}^H\tilde{\mathbf{R}}\mathbf{w}$. The optimal solution to (16) can be directly obtained by using Lemma 1. Please note that, although Lemma 1 only gives a local optimum, it is enough for our algorithm to converge, at least locally. Finally, we summarize the whole algorithm in Algorithm 1.

Algorithm 1

1: **Initialization**: Set arbitrary initial values to $\mathbf{w}_0 \in \mathcal{CM}$, and thresholds $\sigma_1, \sigma_2 \in \mathbb{R}$.
2: **for** $k = 1$ to $k = K$ **do**
3: $\quad \mathbf{w}_c \leftarrow \mathbf{w}_0$
4: $\quad \lambda_{\max} \leftarrow$ the largest eigenvalue of $\mathbf{R}_{\mathrm{I}} - f(\mathbf{w}_c)\mathbf{R}_k$
5: $\quad \tilde{\mathbf{R}} \leftarrow \lambda_{\max}\mathbf{I}_M - (\mathbf{R}_{\mathrm{I}} - f(\mathbf{w}_c)\mathbf{R}_k)$
6: $\quad \mathbf{w}_k \leftarrow e^{j\cdot\arg\left(\tilde{\mathbf{R}}\mathbf{w}_k\right)}$
7: $\quad$ **while** $|f(\mathbf{w}_k) - f(\mathbf{w}_c)| > \sigma_1$ **do**
8: $\quad\quad \mathbf{w}_c \leftarrow \mathbf{w}_k$
9: $\quad\quad$ update $\lambda_{\max}$ according to Step 4
10: $\quad\quad$ update $\tilde{\mathbf{R}}$ according to Step 5
11: $\quad\quad$ update $\mathbf{w}_k$ according to Step 6
12: $\quad\quad$ **while** $|\tilde{g}(\mathbf{w}_k) - \tilde{g}(\mathbf{w}_c)| > \sigma_2$ **do**
13: $\quad\quad\quad$ update $\mathbf{w}_c$ according to Step 8
14: $\quad\quad\quad$ update $\mathbf{w}_k$ according to Step 6
15: $\quad\quad$ **end while**
16: $\quad$ **end while**
17: **end for**

V. Numerical results

In this section, we evaluate the sum rate of a single-cell multiuser massive MIMO system, where the BS, equipped with $M = 30$ antennas, serves $K = 10$ single-antenna users. We take into account the impacts of low precision ADCs and blockers, and compare the sum rates achieved by both fully digital and hybrid BS architectures. For fully-digital system, G-Capon beamformer is used, while for hybrid system, the ABF is obtained according to Algorithm 1, and the DBF is also a G-Capon beamformer which is designed based on the equivalent channel. Hence, we can see the penalty by introducing the additional ABF.

For systems with full-precision ADCs, as shown in Fig. 3, we observe that both fully-digital and hybrid systems are resilient to blockers, which is a direct consequence of our beamformer design criterion. We also notice that our proposed HBF introduces only a small penalty of sum rate, yet saving 66% of the digital chains.

[2] Since $f(\mathbf{w})$ is always lower bounded by 0, convergence is guaranteed.

For a more realistic case, where low-precision ADCs are used in the systems, we see quite different results. When no blockers are in presence, we notice that hybrid systems are more severely affected by the quantization noise than fully-digital systems. This is due to the fact that hybrid systems have much fewer digital chains, which results in a less averaging effect of quantization noise. However, when blockers exist in the system, we observe a very interesting phenomenon: the hybrid system can even outperform a fully-digital system! This seemingly controversial observation arises from the robustness of having a two-step processing. In a fully-digital system, all interference enters the system without any treatment, and as a result the aggregate received signal may contain a large portion of “noise”, whose level maintains after the AGC processing. Effectively, the remaining signal may be heavily corrupted by quantization noise generated by the finite-precision ADCs, such that the SOI becomes difficult to detect. For a hybrid system, however, most impacts of blockers are removed by the ABF. If this is done perfectly, we can expect marginal difference between the blocking and the non-blocking cases in a hybrid system, as we can see in Fig. 3.

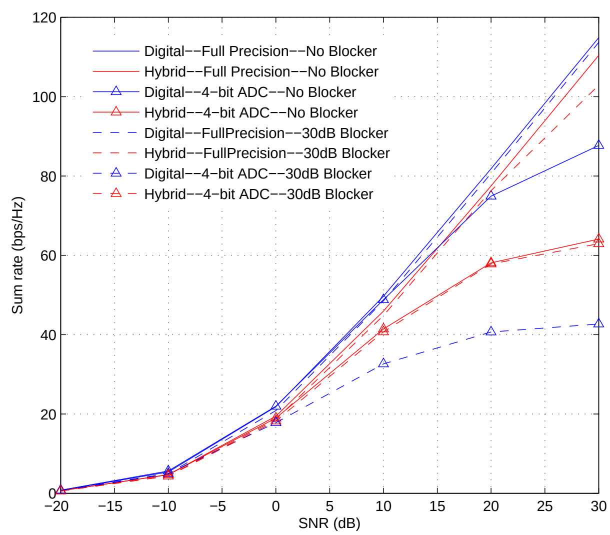

Fig. 3. Sum rates by digital and hybrid beamformers.

VI. Conclusion

In this paper, we considered hybrid beamforming design in uplink massive MIMO systems, in the presence of blockers. Incorporating the impacts of AGC and finite-precision ADCs, we formulated the ABF design as a max-SINR optimization problem, and proposed a two-step iterative algorithm with very good results. In general, our proposed scheme can achieve similar performance compared to fully-digital systems, by using only a small portion of the digital chains. More importantly, we found that, for systems with finite-precision ADCs, fully-digital systems can be heavily corrupted by blockers, while hybrid systems were quite robust. In such a case, hybrid systems can even achieve higher sum rate than fully-digital systems.

REFERENCES

[1] H. Q. Ngo, E. G. Larsson, and T. L. Marzetta, "Energy and spectral efficiency of very large multiuser MIMO systems," *IEEE Trans. Commun.*, vol. 61, no. 4, pp. 1436–1449, Apr. 2013.

[2] O. El Ayach, S. Rajagopal, S. Abu-Surra, Z. Pi, and R. W. Heath, "Spatially sparse precoding in millimeter wave MIMO systems," *IEEE Trans. Wireless Commun.*, vol. 13, no. 3, pp. 1499–1513, 2014.

[3] A. Alkhateeb, O. El Ayach, G. Leus, and R. W. Heath, "Channel estimation and hybrid precoding for millimeter wave cellular systems," *IEEE J. Sel. Topics Signal Process.*, vol. 8, no. 5, pp. 831–846, 2014.

[4] M. Zhang, P. J. Smith, and M. Shafi, "An extended one-ring MIMO channel model," *IEEE Trans. Wireless Commun.*, vol. 6, no. 8, pp. 2759–2764, Aug. 2007.

[5] A. Adhikary, J. Nam, J. Y. Ahn, and G. Caire, "Joint spatial division and multiplexin – the large-scale array regime," *IEEE Trans. Inf. Theory*, vol. 59, no. 10, pp. 6441–6463, Oct 2013.

[6] A. Liu and V. Lau, "Phase only RF precoding for massive MIMO systems with limited RF chains," *IEEE Trans. Signal Process.*, vol. 62, no. 17, pp. 4505–4515, Sep. 2014.

[7] V. Venkateswaran and A.-J. van der Veen, "Analog beamforming in MIMO communications with phase shift networks and online channel estimation," *IEEE Trans. Signal Process.*, vol. 58, no. 8, pp. 4131–4143, 2010.

[8] L. Liang, W. Xu, and X. Dong, "Low-complexity hybrid precoding in massive multiuser MIMO systems," *IEEE Wireless Commun. Lett.*, vol. 3, no. 6, pp. 653–656, 2014.

[9] T. E. Bogale, L. B. Le, and X. Wang, "Hybrid analog-digital channel estimation and beamforming: training-throughput tradeoff," *IEEE Trans. Commun.*, vol. 63, no. 12, pp. 5235–5249, 2015.

[10] J. Mo, A. Alkhateeb, S. Abu-Surra, and R. W. Heath Jr, "Hybrid architectures with few-bit ADC receivers: achievable rates and energy-rate tradeoffs," *arXiv preprint arXiv:1605.00668*, 2016.

[11] M. Soltanalian and P. Stoica, "Designing unimodular codes via quadratic optimization," *IEEE Trans. Signal Process.*, vol. 62, no. 5, pp. 1221–1234, Mar. 2014.

[12] O. Orhan, E. Erkip, and S. Rangan, "Low power analog-to-digital conversion in millimeter wave systems: Impact of resolution and bandwidth on performance," in *Information Theory and Applications Workshop (ITA)*, 2015, pp. 191–198.

[13] D. Araujo, E. Karipidis, A. L. F. de Almeida, and J. C. M. Mota, "Improving spectral efficiency in large-array FDD systems with hybrid beamforming," in *Sensor Array and Multichannel Signal Processing Workshop*, 2015.

[14] A. Hassanien, S. Shahbazpanahi, and A. B. Gershman, "A generalized capon estimator for localization of multiple spread sources," *IEEE Trans. Signal Process.*, vol. 52, no. 1, pp. 280–283, 2004.

[15] Z. Luo, N. D. Sidiropoulos, P. Tseng, and S. Zhang, "Approximation bounds for quadratic optimization with homogeneous quadratic constraints," *SIAM Journal on Optimization*, vol. 18, no. 1, pp. 1–28, Feb. 2007.

[16] A. Barros, J. Frenk, S. Schaible, and S. Zhang, "A new algorithm for generalized fractional programs," *Math. Program.*, vol. 72, pp. 147–175, 1996.